

Semiconductor (SC)-based field-effect transistors (FETs)

Subjects: **Others**

Contributor: Zhe Wang

Semiconductor (SC)-based field-effect transistors (FETs) have been demonstrated as amazing enhancer gadgets due to their delicate interface towards surface adsorption. This leads to their application as sensors and biosensors. Additionally, the semiconductor material has enormous recognizable fixation extends, high affectability, high consistency for solid detecting, and the ability to coordinate with other microfluidic gatherings. This review focused on current progress on the semiconductor-interfaced FET biosensor through the fundamental interface structure of sensor design, including inorganic semiconductor/aqueous interface, photoelectrochemical interface, nano-optical interface, and metal-assisted interface. The works that also point to a further advancement for the trademark properties mentioned have been reviewed here. The emergence of research on the organic semiconductor interface, integrated biosensors with Complementary metal–oxide–semiconductor (CMOS)-compatible, metal-organic frameworks, has accelerated the practical application of biosensors. Through a solid request for research along with sensor application, it will have the option to move forward the innovative sensor with the extraordinary semiconductor interface structure.

biosensor

semiconductor

interface

nanomaterial

field-effect transistor

1. Introduction

The larger part of current biosensors are classified by four distinctive standards. Refinement is a rule determined by affinity, catalytic, transmembrane, and cell sensors. However, the transmembrane and cell sensors are based on affinity or catalytic standards as well. Current investigation and improvement has made strides in sensitivity, selectivity, and stability of biosensors. In particular, there is an expanding drift towards scaling down those spectrometers, chromatographs, and detectors, which are customarily utilized in bioanalytical chemistry, by applying smaller scale- and nano-fabrication procedures. The current biosensors are equipped with miniaturized instruments for clinical application which can be progressively hard to use and, in certain cases, this poses a major challenge, especially, in the study of optical and electroanalytical biosensors. The clinical application of any sensor requires the utilization of total analytic frameworks and consequently integration with sample handling, separation, and even sample conditioning. For designing biosensors, the analysis takes place by coordinate conversion of biochemical information to electronic signal through appropriate transducers and interface. There is a common bottleneck within the advancement of biosensors facing clinical applications that is deficient stability, reproducibility, and sensitivity of their interface properties within the complex clinical samples. Designing the interfaces is the key for next-generation biosensors. Due to a large amount of electrical and optical transducers accessible in thin-film

innovation, most improvements of innovative biosensors aim at the arrangement of a controlled interface structure in which the biomolecular units were organized and packed in a reproducible and controlled manner [\[1\]](#).

Semiconductor-based field-effect transistors (FETs) have attracted critical consideration because of their high delicate interface with fluids, which makes them viable as biosensors [\[2\]](#). A semiconductor additionally has a few qualities, for example, warm affectability, photosensitivity, negative resistivity temperature, rectifiable, etc. In this manner, semiconductor materials can be utilized for control gadgets, optoelectronic gadgets, pressure sensors, thermoelectric refrigeration, and different applications other than assembling enormous scale coordinated circuits. There are numerous orders for sensors, yet there are two usually utilized groupings: one is arranged by the deliberate physical material tested, the other is characterized by the working rule of sensors [\[3\]](#). Sensors arranged by estimated physical amounts are usually temperature sensor, moistness sensor, pressure sensor, uprooting sensor, stream sensor, fluid level sensor, power sensor, speeding up sensor, torque sensor, and so on [\[4\]](#)[\[5\]](#)[\[6\]](#)[\[7\]](#)[\[8\]](#)[\[9\]](#)[\[10\]](#)[\[11\]](#)[\[12\]](#)[\[13\]](#)[\[14\]](#)[\[15\]](#)[\[16\]](#)

2. Current Progress Semiconductor Interfaced-Based Field-Effect Transistor (FET) Biosensors

2.1. Inorganic Semiconductor/Aqueous Interface

The many pathways of enhancing the sensing characteristics of metal oxides and metal sulfide by optimizing various parameters, such as synthesis methods, morphology, composition, and structure, have been explored in the last 10 years. For example, TiO_2 , ZnO , SnO_2 , and WO_3 , has been presented based on several aspects: synthesis method, morphology, functionalizing molecules, detection target, and limit of detection (LOD) [\[17\]](#)[\[18\]](#)[\[19\]](#). Various developments have been made regarding applications of a metal oxide semiconductor (MOS)-based biosensors for environmental and biological systems. The recent developments have been summarized by the Enesca group in a concessive overview of the applications of metal oxides [\[20\]](#). This describes the optimization of certain parameters for enhancing the sensing property of MOS. The parameters discussed include the method of synthesis, composition, structure, and morphology. Based on the aspects such as optimization of synthesis protocols, functionalizing agents, morphology, target detection, and limit of detection (LOD), the new representative metal oxides including TiO_2 , MoS_2 , graphene, and WSe_2 with novel engineered methods are presented in this work. For the interface characterization, X-ray photoelectron spectroscopy (XPS) and ultraviolet photoelectron spectroscopy (UPS) have been widely used for investigating a wider range of organic–organic and metal–organic semiconductor interfaces [\[20\]](#). Hill et al. [\[21\]](#), reported the use of UPS for the determination of binding energies associated with vacuum level position and highest occupied molecular orbital. Furthermore, they used UPS confirmation of possible chemical interaction that occurred at heterointerfaces. They found that most organic–organic interfaces exhibited the aligned vacuum level (with some exceptions), while all metal–organic interfaces exhibited strong interface dipoles which were responsible for an abrupt offset of the vacuum level. Moreover, the presence of dipoles in the metal–organic semiconductor interfaces where the Fermi level was completely unpinned within the gaps of semiconductors. This suggested that dipoles were not dependent on emptying or populating Fermi level-pinning gap states [\[21\]](#).

2.2. Photoelectrochemical Biosensors

In photoelectrochemistry, light is utilized to produce electron/opening sets in a photoactive material, and these electron/gap sets, when isolated, are utilized to drive redox responses. Contingent upon the responses happening in the photoelectric compound (PEC) cell, light is then changed over to electrical or synthetic energy. Recently, PEC signal transduction has been exhibited for organic detecting. In PEC biosensors, light is utilized to create charge transporters in photoactive materials, and the transduced electrochemical current is estimated for examining naturally significant targets. Since signal readout is electrochemical, this technique acquires the advantages of electrochemical biosensing:

- The sign is perused utilizing economical and simple to-utilize instrumentation.
- Multiplexed location is accomplished utilizing multielectrode microchips.
- Due to optical excitation, PEC estimations are performed at lower inclination possibilities contrasted with their electrochemical partners.
- This brings down the deliberate electrochemical foundation flows and builds the sign-to-foundation proportion. PEC readout has been utilized to identify biomolecules, for example, DNA, RNA, and proteins. In any case, when utilizing these creation techniques, the compromise must be made between the level of auxiliary tunability, throughput, and cost.

The gathering utilized surface wrinkling to upgrade the proficiency of photocurrent age in detecting PEC cells. Surface wrinkling is a simple and economical technique for bringing tunable smaller scale and nanostructuring into dainty movies, permeable systems, and get together of nanoparticles. In this work, The Soleymani group devised a strategy for stacking photoactive quantum dots (QDs) into a wrinkled platform of a straightforward conductive oxide to improve the produced photocurrent ([Figure 1](#)). By functionalizing the photoactive QDs implanted in the wrinkled film, we built up a sensor for distinguishing DNA targets. The wrinkles were made legitimately on polystyrene by shaping a hardened oxidized surface layer and contracting the substrate. The indium tin oxide (ITO) and QDs were then sputtered and stacked into the wrinkled polystyrene framework, separately. The distinctions in surface geology and progression between the three classes of photoelectrodes. The standard photoelectrodes are planar, and their ITO layer was free of breaks. These components, which the article talked about, additionally empowered the oxidized layer to adjust instead of break in light of the applied strain, making a continuous wrinkled layer, and afterward, PEC current for the scaffolded-wrinkled surface (at 3 layers) was around multiple times bigger than the current accomplished in the planar surface. The stem was utilized to think about the PEC current pattern and as the charges travel through the system of QDs and the PDDA (poly (diallyl dimethylammonium chloride)) spacer, resistive misfortunes, dispersion misfortunes, and recombination decline their gathering rate by the ITO anode, further lessening the photograph current. The gathering explored the progressions in PEC current when the scaffolded-wrinkled photoelectrodes were interfaced with test and target DNA strands. The upgraded PEC current

acquired utilizing the wrinkled materials design empowered us to build up a delicate and mark-free DNA biosensor with a picomolar limit-of-detection [22].

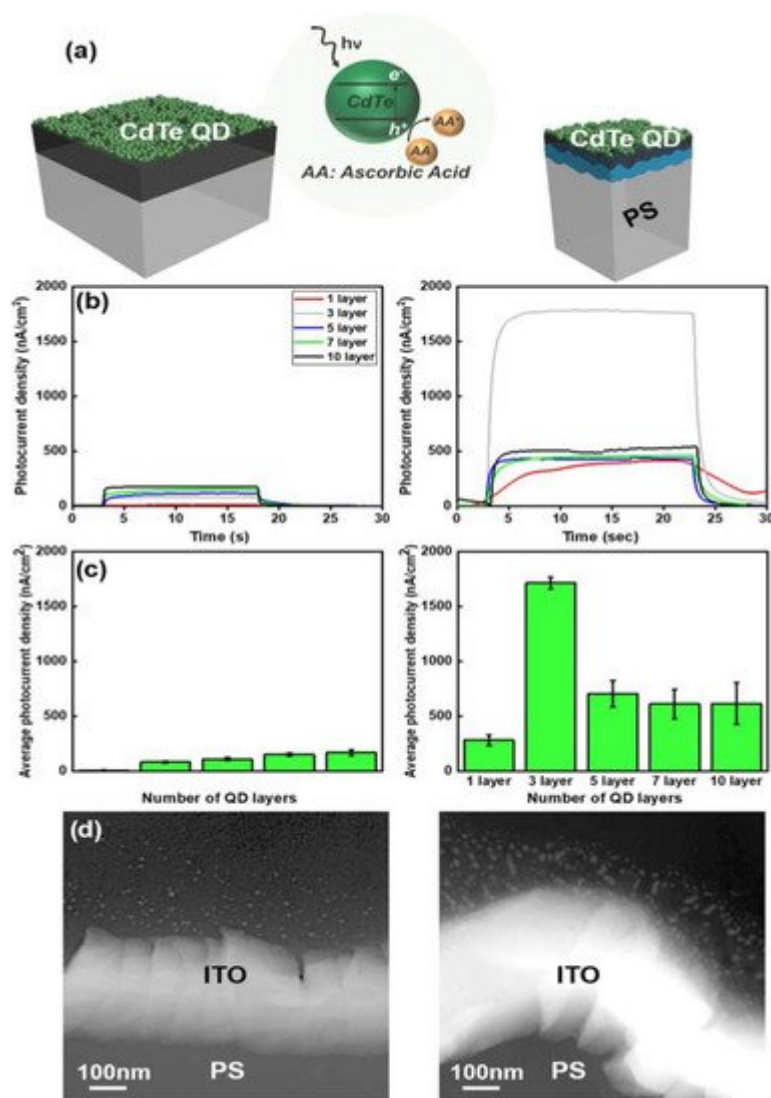


Figure 1. Photoelectric compound (PEC) measurements at planar and scaffolded-wrinkled photoelectrodes. (a) Visible light (470 nm) induces electron/hole pairs in CdTe quantum dots (QDs). Holes oxidize ascorbic acid, generating an anodic redox current. (b) PEC current densities measured on planar (**left**) and scaffolded-wrinkled (**right**) devices using 100 mM ascorbic acid at 0 V with respect to Ag/AgCl. The QD layers are increased by depositing alternate layers of QDs and poly (diallyl dimethylammonium chloride) (PDDA). The 470 nm light-emitting diode is turned on at 3 s and turned off at 23 s. (c) The average PEC current densities measured on planar (**left**) and scaffolded-wrinkled (**right**) devices for different numbers of QD layers. (d) Scanning transmission electron micrographs of cross-sections of planar (**left**) and scaffolded-wrinkled (**right**) devices. The imaged devices contain three QD layers. Reprinted with permission from ref. [22]. 2018 American Chemistry Society.

Zhang et al. [23], reported the design and development of a self-operating photocathode which was based on the CdS quantum dots sensitized with 3D nanoporous-NiO ([Figure 2](#)). The photocathode reversibly exhibited high selectivity towards dissolved oxygen (working as electron donor) in the electrolyte solution. Employing the

photocathode, a novel photoelectrochemical sensor was developed for the detection of glucose while using glucose oxidase (GOD) as a biocatalyst. The use of various competing substances such as dopamine (DA), cysteine (Cys), ascorbic acid (AA), and H_2O_2 revealed that they did not affect the cathodic photocurrent of the 3D NiO/CdS electrode. However, they significantly influenced the photocurrent of the photocathode, thus authenticating the selectivity of the described method.

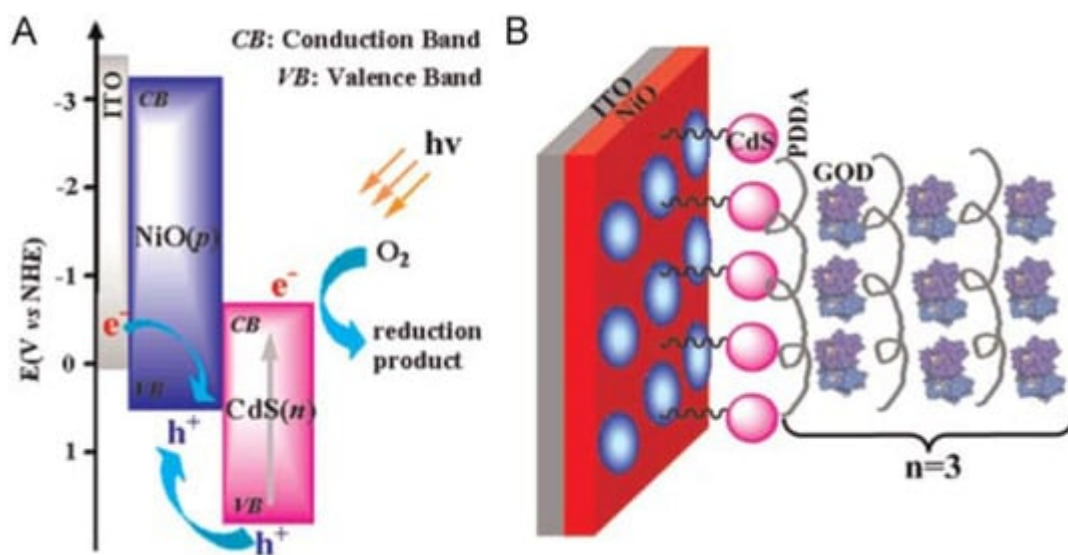


Figure 2. (A) Schematic diagrams for energy bands of n-CdS and p-NiO and photocurrent generation mechanism of NiO/CdS in the presence of oxygen. (B) The assembly of glucose oxidase (GOD) on indium tin oxide (ITO)/NiO/CdS Selectrode. Reprinted with permission from ref. [23]. 2014 ScienceDirect.

The applicability of the method was investigated for the detection of glucose present in real samples including glucose injection and blood serum. The obtained results showed they were highly satisfactory in terms of accuracy. The authors of the study concluded that these findings could open new avenues for designing and developing photochemical biosensors based on self-operating photocathode, and this would, in turn, promote the applications of semiconductor nanomaterials in photoelectrochemistry. The further report showed the design and development of a self-operating photocathode which was based on the CdS quantum dots sensitized with 3D nanoporous-NiO. The photocathode reversibly exhibited high selectivity towards dissolved oxygen (working as electron donor) in the electrolyte solution. Employing the photocathode, a novel photoelectrochemical sensor was developed for the detection of glucose while using glucose oxidase (GOD) as a biocatalyst. The use of various competing substances such as dopamine (DA), cysteine (Cys), ascorbic acid (AA), and H_2O_2 revealed that they did not affect the cathodic photocurrent of the 3D NiO/CdS electrode. However, they significantly influenced the photocurrent of the photocathode, thus authenticating the selectivity of the described method [23].

Zheng et al. [24] reported the synthesis of a novel sensor for the detection of glucose (Figure 3). The sensor was based on single-crystalline TiO_2 nanowires that were synthesized through a hydrothermal synthetic route. The nanowires were further surface-functionalized with glucose oxidase, and enzymes responsible for the oxidation of glucose to gluconic acid. The development of the sensor was based on the photogenerated holes on the TiO_2

anode surface that could generate O_2 . Thus, the O_2 was considered responsible for the efficient shuttling mediator of electron between the surface of the sensor and the redox center of glucose oxidase. This in turn resulted in significant photocurrent enhancement. The surface-functionalized nanowire-based sensor was found to be highly sensitive towards glucose in buffer with an as low as ~ 0.9 nM lower limit of detection. The sensor was further investigated for its glucose detection capability in complex system mouse serum. The authors concluded the novel nanowire-based photoelectrochemical sensor as an efficient, convenient, and cost-effective diagnostic for the detection of disease biomarkers [24]. The Tang report that PEC biosensors have been used for mycotoxin detection due to their properties. Photoactive materials like this have important roles in converting chemical information into detectable PEC signal. Specific recognition elements also affect the analytical performance of PEC biosensors [25].

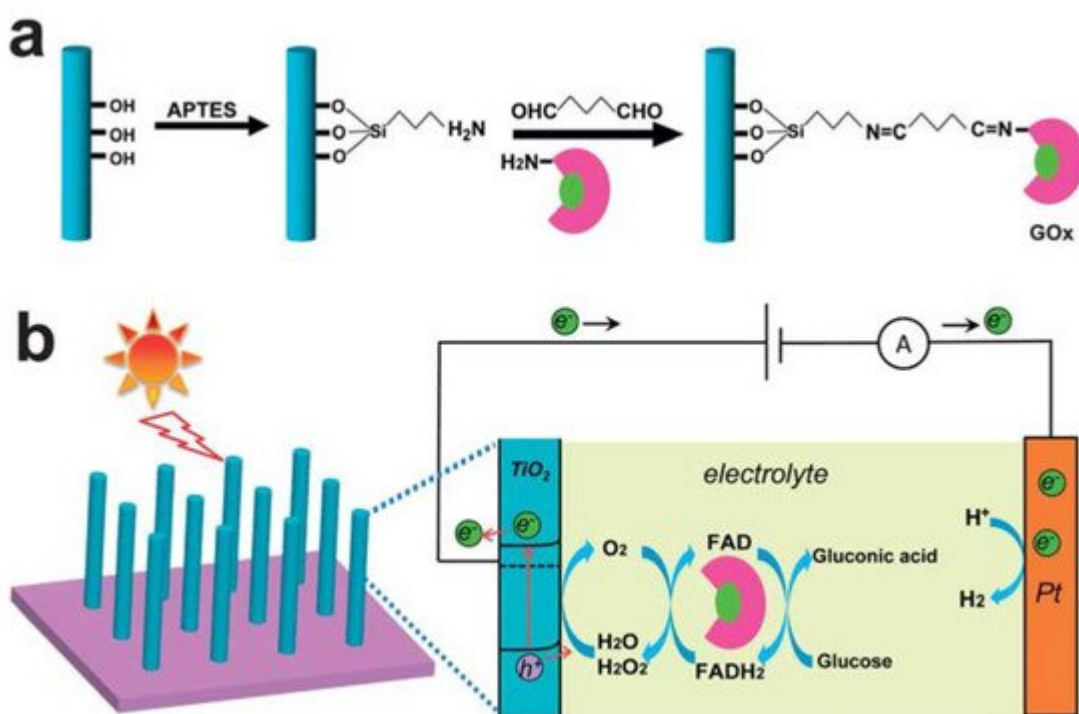


Figure 3. (a) Schematic of glucose oxidase (GOx) functionalization on the TiO₂ nanowire surface via silane/glutaraldehyde linkage chemistry. APTES: 3-aminopropyl triethoxysilane. The green and pink colors of GOx indicate the flavin group (FAD) redox center and the external insulating protein shell, respectively. (b) Schematic of the TiO₂-GOx NW-based PEC sensor for glucose detection. Under sunlight illumination, the photogenerated holes oxidize H₂O or H₂O₂ over the TiO₂NW anode to form O₂, which serves as an efficient electron acceptor of FAD/FADH₂. Glucose is oxidized to gluconic acid during this cycle. On the cathode (Pt), the photogenerated electrons reduce water to form H₂. The current flowing through the circuit is recorded as the sensing signal. Reprinted with permission from ref. [24]. 2013 The Royal Society of Chemistry.

Photoelectrochemical detection of analytes is greatly preferred as it presents an interesting signal transduction modality. Modulation of the charge carriers in such sensing systems occurs as a result of the redox reactions of molecular targets that take place on the surface of the electrode. Owing to the superior properties of PEC biosensors, they are considered to be used as a promising tool for the detection of mycotoxin. When employed in the fabrication of biosensing systems, photoactive materials work as transducers, thus they convert the chemical

information into detectable signals. The analytical performance of biosensors based on PEC materials is greatly influenced by the signal strategies of the specific recognition element. A review by Tang et al. extensively reviewed the photoactive materials and their signal strategies employed for the fabrication of PEC biosensors used for the detection of mycotoxin. They also discussed the future aspects of these biosensors in detail.

2.3. Nano Optical Biosensor

Nanoscale optical biosensors are currently attracting greater scientific interest due to their easy fabrication, characterization, and cost-effectiveness. The Duyne group [26] reported the usage of nano-sphere lithography (NSL) for the fabrication of gold and silver nano-triangles and the resulting localized surface plasmon resonance (LSPR) spectra were recorded by using ultraviolet (UV)–Visible extinction spectroscopy. They found that the short-range distance dependence (almost 0–2 nm) of electromagnetic fields surrounding the resonantly excited nanoparticles can be modulated through varying their structure, composition, and size. The measurement was based on shifting of LSPR spectra wavelengths (λ_{max}) that appeared due to the absorption of hexadecane-thiol as a function of nanoparticle shape (truncated tetrahedron versus hemisphere), size (in-plane width, out-of-plane height, and aspect ratio) and composition (silver versus gold). It was observed that hexadecane-thiol-induced LSPR shift for silver triangles decreased with an increase in width (in-plane) at a fixed height (out-of-plane) or vice versa. The described trends were in contrast to the findings of the previously published report which studied long-range distance dependence examining layers with 30 nm thickness [26]. However, the confirmation of these results for both short and long-range analysis was based on theoretically using finite element electrodynamics. Findings of the study revealed that short-range distance-dependence results were found sensitive to hot spots (these are the regions having highly induced electric fields) located in peripheries of the triangles, and hence they suggested the involvement of enhanced local fields for the generation of extinction spectra. The results also exhibited the appearance of larger hexadecane thiol-induced LSPR peak shifts in the case of nano triangles as compared to hemispheres of the same volume. Similarly, a larger peak shift was observed for the silver nano-triangles as compared to gold nano-triangles having the same out-of-plane heights and in-plane widths. It was also found that alkane-thiol-induced LSPR peak shift of chain-length present in silver nano triangles was independent of the size. A better understanding of the reported short-range dependence of the adsorbate-induced LSPR peak shift associated with nanoparticle composition as well as structure will provide knowledge to improve the sensitivity of nanosensors based on refractive-index [27].

Nano-silicon photonics is an ideal stage to realize high orthodontic and selective recognition of organic atoms under complex fluid conditions. In this case, luminescent silicon-based nanostructures are very encouraging materials because their large uncoated surfaces and their optical properties are due to the most innovative conduction techniques. In the aspect of DNA recognition, the basic detection of Si-nws was carried out by using the electric conduction strategy based on DNA hybridization conductance variation and the explicit detection method fixed on the surface of nanowires (NWs), and 220 atoms (about 6600 DNA target duplicates per 50 mL) that were low fracture points were found. SSDNA, by using a variety of crystal silicon nano-FETs with measurements of less than 20 nm, another interesting approach relies on fluorescent labeling of DNA. In particular, his collection demonstrates the high performance of Si NWs biochemical sensors to reduce the identification of various named

genome sequences to as low quality as possible. Sabrinas' [28] collections reported major cases of direct genomic identification in Si-NWs optical biosensors without enhancement steps (sans-pcr) and markers (unlabeled) (Figure 4). The proposed approach utilizes a hybrid approach that combines Si NWS with satisfactory in situ hybridization from two explicit experiments and synthesizes it on the surface with a genomic double strand. We tried to demonstrate sensors that take advantage of the hepatitis b virus (HBV) genome. Figure 4a the concentrations range from 20 cps to 2000 cps for the Photoluminescence (PL) spectra of the NWs sensor that was tested in HBV genome extraction from infected human blood. The PL reference of the sensor without any copies of HBV is depicted in black. Figure 4b shows that the PL integrated peak of the NWs PL emission is obtained by the buffer solution without any real HBV copy. Lastly, the PL signal is used as a detection mechanism.

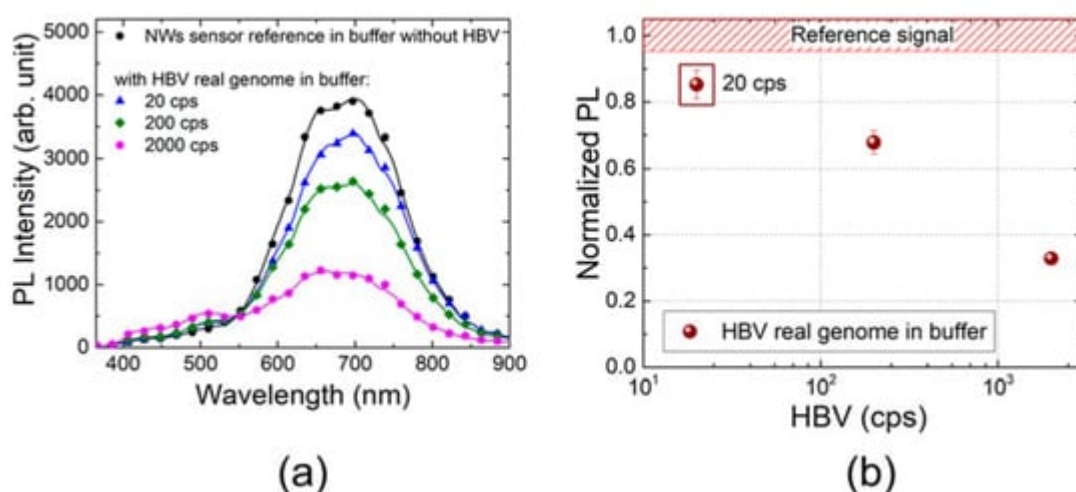


Figure 4. (a) Photoluminescence (PL) spectra of the NWs sensor tested in hepatitis b virus (HBV) real genome extracted from infected human blood and spiked in buffer reported for different concentrations ranging from 20 cps up to 2000 cps. The PL reference of the sensor without any copies of HBV is shown in black. (b) The trend of the PL integrated peak of the deconvolved NWs PL emission as a function of real HBV genome concentration normalized to its reference signal (red bar) obtained by the buffer solution without any real HBV copy. Reprinted with permission from ref. [28]. 2018 American Chemistry Society.

The impact of a natural network and its potential impediments can be evaluated by testing the Si NWS sensor with HBV clone genome broke up in human serum rather than the support arrangement. To affirm this theory, a Si wafer (without NWS) was tried with an answer made by human serum without HBV, and a similar wide multipeaked band 400–600 nm was watched and verified that the PL signal variety of the NWs sensor as a component of HBV focus is the equivalent in the two grids. The presentation evaluation of the Si NWS sensor with genuine examples is a significant point to be tended to. To further explore this point, we tried the gadget by utilizing a genuine HBV genome removed from a blood test. It was affirmed that this Si NWS sensor can distinguish the genuine HBV genome separated from human blood with an effectiveness similar to the constant PCR (20 cps/response), regardless of whether its length is about the portion of the analytical sample [29].

The Duyne group reported the usage of NSL for the fabrication of gold and silver nano-triangles and the resulting LSPR spectra were recorded by using UV-Visible extinction spectroscopy. They found that the short-range distance dependence (almost 0–2 nm) of electromagnetic fields surrounding the resonantly excited nanoparticles can be modulated through varying their structure, composition, and size. The measurement was based on shifting of LSPR spectra wavelength (λ_{max}) appeared due to the absorption of hexadecane-thiol as a function of nanoparticle shape (truncated tetrahedron versus hemisphere), size (in-plane width, out-of-plane height, and aspect ratio) and composition (silver versus gold). It was observed that hexadecane-thiol-induced LSPR shift for silver triangles decreased with an increase in width (in-plane) at a fixed height (out-of-plane) or vice versa. The described trends were in contrast to the findings of the previously published report which studied long-range distance dependence examining layers with 30 nm thickness [26]. However, the confirmation of these results for both short and long-range analysis was based on theoretically using finite element electrodynamics. Findings of the study revealed that short-range distance-dependence results were found to be sensitive to hot spots (these are the regions having highly induced electric fields) located in peripheries of the triangles, hence suggested the involvement of enhanced local fields for the generation of extinction spectra. The results also exhibited the appearance of larger hexadecane thiol-induced LSPR peak shifts in the case of nano triangles as compared to hemispheres of the same volume. Similarly, a larger peak shift was observed for the silver nano-triangles as compared to gold nano-triangles having the same out-of-plane heights and in-plane widths. It was also found that the alkane-thiol-induced LSPR peak shift of chain-length present in silver nano triangles was independent of the size. A better understanding of the reported short-range dependence of the adsorbate-induced LSPR peak shift associated with nanoparticle composition as well as structure will provide knowledge to improve the sensitivity of nanosensors based on refractive-index [27].

2.4. Metal-Assisted Interface

Plasma biosensors are widely used in logic and medicine research, medical diagnosis, veterinary practice, nutrition, and health control. Stebunovs et al. [30] collects copper as a plasma material for constructing biosensor interfaces. (Figure 5) One potential way to overcome this problem is to protect the hidden metal surface with a graphene-covered barrier while having a negligible effect on the optical properties of the interface between the sensor surface and the substance to be tested or the organic frame. Stebunovs' team proposed the SPR sensor chip, which relies on plasma-copper membranes fixed with different dielectric layers (Figure 6). The disappearance of the electron column is an essential part of the standard process, which stores thin copper film on the surface of the glass substrate. The optical properties of the metal film determine the probability of SPR excitation in a specific structure, the reverberation quality, and the feasibility of SPR biosensors. The ellipsoidal model shows that the dielectric constants of copper and gold films are directly determined by the ellipsoidal information. The variation of copper SPR sensor chips with different protective layers is hypothesized and preliminarily tested. Improvement with the ligand-specific interface in SPR biosensing applications analysis is important because 2D material has large surface area and different material properties, and the interface can be applied to a wide range of biological chemical association study, no matter under what circumstances, compared with sulfur connection layer, increasing the limit immobilized. This recent report showed the progress of the go connection layer covering the dielectric layer outside the SPR biosensor chip [29]. The Chang group proposed and validated a highly sensitive metal layer-assisted guide mode resonance (MaGMR) device for use in bioanalytical contexts. These researchers found that

reflection spectra associated with this approach presented a unique inverse response, and were able to explore the underlying mechanistic basis for observed resonance. The high sensitivity of their MaGMR device was found to be attributable to its asymmetric resonance model profile and the low propagation angle inside the waveguide. Relative to typical GMR, these researchers observed a 1-fold enhancement of the evanescent waves within the analyte region. In experimental analyses, they found that the MaGMR was able to achieve a bulk sensitivity of 376.78 nm in fundamental TM mode while resonating at 0.809 μ m with the first diffraction angle. They observed a 264.78% enhancement in the sensitivity relative to typical GMR sensors under identical TM mode resonance conditions [31].

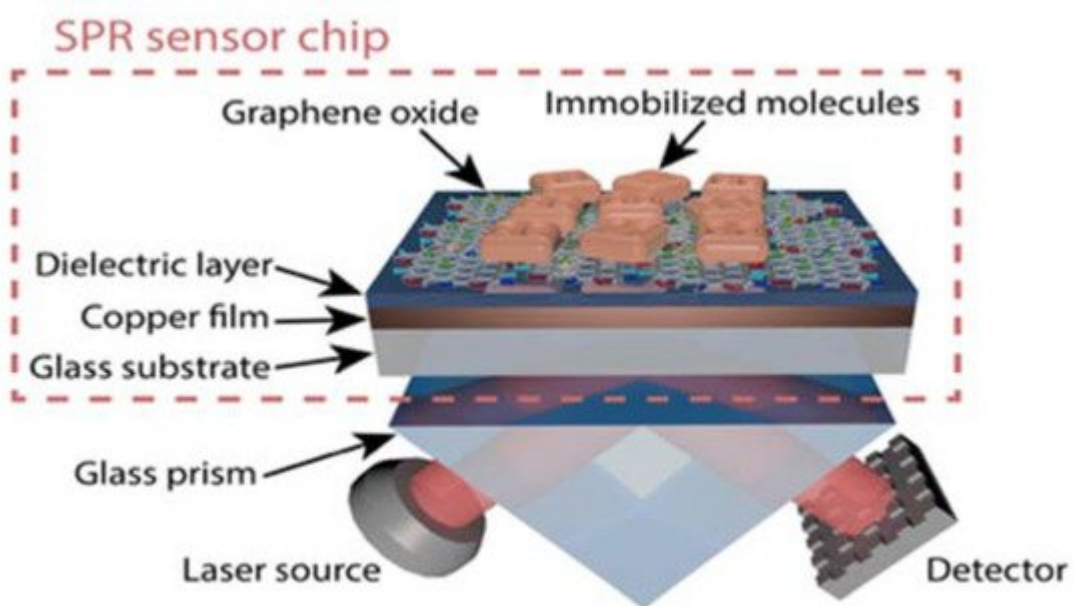


Figure 5. Schematic representation of the surface plasmon resonance (SPR) biosensor comprising the SPR sensor chip based on plasmonic copper films coated with a dielectric layer to protect against oxidation. The prism and sensor chip substrates are made of the same type of glass, which allows for an efficient optical connection. The immobilization of biomolecules on the biosensor surface can be achieved using a graphene oxide linking layer deposited atop the dielectric layer. Reprinted with permission from ref. [30]. 2018 American Chemistry Society.

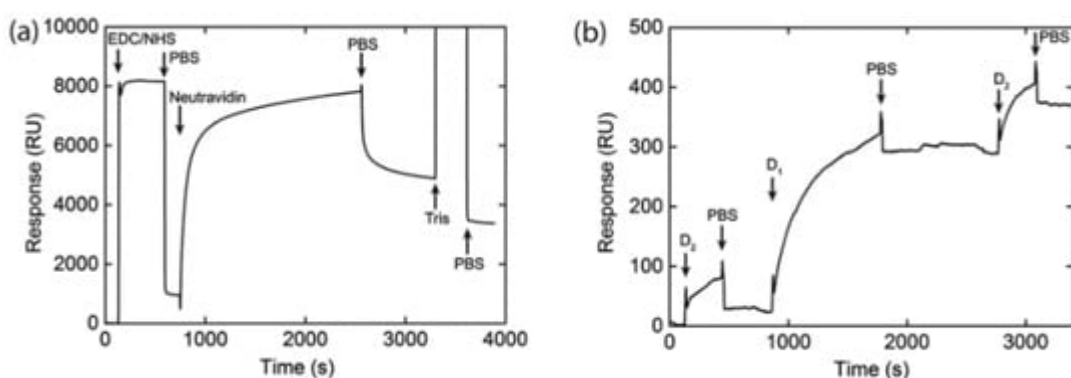


Figure 6. (a) Covalent immobilization of neutravidin on the surface of the graphene oxide (GO) linking layer deposited on the copper surface plasmon resonance (SPR) sensor chip protected by 15 nm thick Al_2O_3 film. The immobilization procedure includes the activation of carboxyl groups of GO by the mixture of 0.4 M 1-ethyl-3-(3-(dimethylamino) propyl) carbodiimide hydrochloride (EDC) and 0.1 M N-hydroxysuccinimide (NHS) solutions and deactivation of carboxyl groups after neutravidin adsorption by 1 M Tris solution. (b) Adsorption of oligonucleotides D1 and D2 on the surface of neutravidin–GO copper SPR chip. D1 is biotinylated and complementary to non-biotinylated D2. PBS: phosphate-buffered saline Reprinted with permission from ref. [30]. 2018 American Chemistry Society.

References

1. Göpel, W.; Heiduschka, P. Interface analysis in biosensor design. *Biosens. Bioelectron.* 1995, 10, 853–883.
2. Sarkar, D. Chapter 9—2D materials for field-effect transistor–based biosensors. In *Fundamentals and Sensing Applications of 2D Materials*; Hywel, M., Rout, C.S., Late, D.J., Eds.; Woodhead Publishing: Cambridge, UK, 2019; pp. 329–377.
3. Chi, E.H. Introducing wearable force sensors in martial arts. *IEEE Pervasive Comput.* 2005, 4, 47–53.
4. Akyildiz, I.F.; Weilian, S.; Sankarasubramaniam, Y.; Cayirci, E. A survey on sensor networks. *IComM* 2002, 40, 102–114.
5. Yick, J.; Mukherjee, B.; Ghosal, D. Wireless sensor network survey. *Comput. Netw.* 2008, 52, 2292–2330.
6. Martinez, K.; Hart, J.K.; Ong, R. Environmental sensor networks. *Computer* 2004, 37, 50–56.
7. Wilson, J.S. *Sensor Technology Handbook*; Elsevier: Burlington, MA, USA, 2004.
8. Vadgama, P.M.; Higson, S.P. Sensor Devices. U.S. Patent 5531878A, 2 July 1996.
9. Ahl, T.; Byrnard, A.M. Enzyme Sensor. U.S. Patent 6051389A, 18 April 2000.
10. McIvor, K.C.; Cabernoch, J.L.; Branch, K.D.; Van Antwerp, N.M.; Halili, E.C.; Mastrototaro, J.J. Glucose sensor package system. US6892085B2, 10 May 2005.
11. Chee-Yee, C.; Kumar, S.P. Sensor networks: Evolution, opportunities, and challenges. *Proc. IEEE* 2003, 91, 1247–1256.
12. Wang, G.; Cao, G.; Porta, T.F.L. Movement-assisted sensor deployment. *IEEE Trans. Mob. Comput.* 2006, 5, 640–652.
13. Hu, L.; Evans, D. Localization for mobile sensor networks. In *Proceedings of the 10th Annual International Conference on Mobile Computing and Networking*, Philadelphia, PA, USA, 26

Septembre–1 October 2004; pp. 45–57.

14. Shostak, O.T.; Kolomeyko, A.V.; Breed, D.S.; Duvall, W.E.; Johnson, W.C. Sensor Assemblies. U.S. Patent 7089099B2, 8 August 2006.

15. Madou, M.J.; Otagawa, T. Microelectrochemical sensor and sensor array. U.S. Patent 4874500A, 17 October 1989.

16. Feng, Z.; Jaewon, S.; Reich, J. Information-driven dynamic sensor collaboration. ISPM 2002, 19, 61–72.

17. Foresti, M.L.; Vázquez, A.; Boury, B. Applications of bacterial cellulose as precursor of carbon and composites with metal oxide, metal sulfide and metal nanoparticles: A review of recent advances. *Carbohydr. Polym.* 2017, 157, 447–467.

18. Korotcenkov, G. The role of morphology and crystallographic structure of metal oxides in response of conductometric-type gas sensors. *Mater. Sci. Eng. R. Rep.* 2008, 61, 1–39.

19. Shankar, P.; Rayappan, J.B.B. Gas sensing mechanism of metal oxides: The role of ambient atmosphere, type of semiconductor and gases-A review. *Sci. Lett. J.* 2015, 4, 126.

20. Șerban, I.; Enesca, A. Metal oxides-based semiconductors for biosensors applications. *Front. Chem.* 2020, 8, 354.

21. Hill, I.G.; Milliron, D.; Schwartz, J.; Kahn, A. Organic semiconductor interfaces: Electronic structure and transport properties. *ApSS* 2000, 166, 354–362.

22. Saha, S.; Chan, Y.; Soleymani, L. Enhancing the Photoelectrochemical Response of DNA Biosensors Using Wrinkled Interfaces. *ACS Appl. Mater. Interfaces* 2018, 10, 31178–31185.

23. Wang, G.-L.; Liu, K.-L.; Dong, Y.-M.; Wu, X.-M.; Li, Z.-J.; Zhang, C. A new approach to light up the application of semiconductor nanomaterials for photoelectrochemical biosensors: Using self-operating photocathode as a highly selective enzyme sensor. *Biosens. Bioelectron.* 2014, 62, 66–72.

24. Tang, J.; Wang, Y.; Li, J.; Da, P.; Geng, J.; Zheng, G. Sensitive enzymatic glucose detection by TiO₂ nanowire photoelectrochemical biosensors. *J. Mater. Chem. A Mater.* 2014, 2, 6153–6157.

25. Zhou, Q.; Tang, D. Recent advances in photoelectrochemical biosensors for analysis of mycotoxins in food. *TracTrends Anal. Chem.* 2020, 124, 115814.

26. Haes, A.J.; Zou, S.; Schatz, G.C.; Van Duyne, R.P. A nanoscale optical biosensor: The long range distance dependence of the localized surface plasmon resonance of noble metal nanoparticles. *J. Phys. Chem. B* 2004, 108, 109–116.

27. Haes, A.J.; Zou, S.; Schatz, G.C.; Van Duyne, R.P. Nanoscale optical biosensor: Short range distance dependence of the localized surface plasmon resonance of noble metal nanoparticles. *J.*

Phys. Chem. B 2004, 108, 6961–6968.

28. Leonardi, A.A.; Lo Faro, M.J.; Petralia, S.; Fazio, B.; Musumeci, P.; Conoci, S.; Irrera, A.; Priolo, F. Ultrasensitive Label- and PCR-Free Genome Detection Based on Cooperative Hybridization of Silicon Nanowires Optical Biosensors. *ACS Sens.* 2018, 3, 1690–1697.

29. Uemura, T.; Hirahara, R.; Tominari, Y.; Ono, S.; Seki, S.; Takeya, J. Electronic functionalization of solid-to-liquid interfaces between organic semiconductors and ionic liquids: Realization of very high performance organic single-crystal transistors. *ApPhL* 2008, 93, 263305.

30. Stebunov, Y.V.; Yakubovsky, D.I.; Fedyanin, D.Y.; Arsenin, A.V.; Volkov, V.S. Superior Sensitivity of Copper-Based Plasmonic Biosensors. *Langmuir* 2018, 34, 4681–4687.

31. Lin, S.-F.; Wang, C.-M.; Ding, T.-J.; Tsai, Y.-L.; Yang, T.-H.; Chen, W.-Y.; Chang, J.-Y. Sensitive metal layer assisted guided mode resonance biosensor with a spectrum inversed response and strong asymmetric resonance field distribution. *OExpr* 2012, 20, 14584–14595.

Retrieved from <https://encyclopedia.pub/entry/history/show/24787>